Progress In Electromagnetics Research B, Vol. 15, 95–112, 2009

DESIGN AND ANALYSIS OF WIDEBAND PLANAR MONOPOLE ANTENNAS USING THE MULTILEVEL FAST MULTIPOLE ALGORITHM

Y. Chen, S. Yang, S. He, and Z. Nie

Department of Microwave Engineering
School of Electronic Engineering
University of Electronic Science and Technology of China (UESTC)
Chengdu 610054, China

Abstract—Two planar monopole antennas with wide impedance bandwidth are designed. A full-wave method of moment (MoM) based on the electric field integral equation (EFIE) is applied to analyze the impedance bandwidth and radiation performance of the monopoles. Meanwhile, the multilevel fast multipole algorithm (MLFMA) is employed to reduce the memory requirements and computational time. Experimental results such as the impedance bandwidth and radiation patterns are also presented. The good agreement between the experimental and numerical results well demonstrates the efficiency and accuracy of the MLFMA code. Both the experimental and numerical results show that the two planar monopole antennas possess good input impedance and radiation performance over the AMPS, GSM900, and DCS band. As the proposed antennas can achieve such wide impedance bandwidth with relatively low profile, they are very suitable for multi-band mobile communication systems.

1. INTRODUCTION

The increasing demand for wireless communication systems spurs on the need for antennas capable of operating at a wide frequency band. Owing to their attractive merits such as simple structure, pure polarization, and omnidirectional radiation pattern, the conventional monopole and its variants have been widely used in wireless communications. However, their inherent narrow bandwidth has been a setback to be overcome in broadband applications. Moreover, the

Corresponding author: S. Yang (swnyang@uestc.edu.cn).

vertical monopole antenna has a relatively large height of $\lambda/4$, thus it is not recommended when a low profile is desired. To realize a monopole-like radiation pattern with low profile and relatively wide bandwidth, an alternative approach that makes use of the higher order modes of circular or annular-ring microstrip antennas has been developed [1–3]. The microstrip antenna designs usually suffer from a narrow impedance bandwidth (typically 30–50%) because of its high-Q resonant feature. Recently, another approach that makes use of the diffractions of surface waves at the ground plane boundary is proposed to obtain a monopole-like pattern [4, 5]. This type of surface wave antenna only requires a low profile of 0.05λ. However, experimental results showed that the impedance bandwidth is rather limited (only about 6%). The above two kinds of designs cannot meet the demands of multi-band wireless communication systems.

Recently, extensive research has focused on the development of low profile monopole antennas that have wide enough impedance bandwidth to cover several operating frequency bands of wireless communication systems (e.g., AMPS: 824–894 MHz, GSM900: 890–960 MHz, DCS: 1710–1880 MHz, etc.). Planar monopole antennas have arisen as an interesting design due to their wideband matching characteristic, omnidirectional radiation pattern, high radiation efficiency, and compact size. The square planar monopole antenna with very wide impedance bandwidth was first reported by Dubost and Zisler [6] in 1976. Later, circular planar monopoles were introduced for wideband applications [7–9]. The favorable features of wideband planar monopole antennas have attracted many studies. Techniques such as adding shorting posts [10–12], beveling technique [10, 13, 14], rounding the lower edge [15, 16], double-feed technique [17] and use of trident-shaped feeding strip [18] are developed to enhance the bandwidth performance and reduce the antenna height. Other interesting designs such as orthogonal square monopole [19], roll monopole [20], and U-shaped monopole [21] are also developed to avoid poor omnidirectional radiation characteristics at higher frequencies.

In this article, two compact planar monopole antennas for potential wireless communication applications operating at AMPS, GSM900, and DCS band are designed, analyzed, and measured. On the other hand, one may note that there has been no simple model emerged to explain the behavior of planar monopoles, so a full wave computer analysis is essential both for understanding their wide bandwidth capabilities and for predicting poor radiation performances at higher frequencies. The problem of a monopole connected to a ground plane has been numerically investigated in several studies. Hybrid techniques combining moment method with the geometrical theory of diffraction

(GTD) have been developed in [22, 23] to calculate the input impedance of monopoles mounted on a finite ground plane. A moment method has been employed in [24, 25] for the analysis of monopoles located at the center of a circular disk, in which the circular disk is divided into concentric circular annular zones. The method of moment (MoM) is then extended for the analysis of monopoles positioned arbitrarily over the finite ground plane [26]. The heavy computational burden MoM carried will limit its applicability to electrically large problems, thus it is usually combined with high frequency techniques such as GTD to solve large-scale EM problems, but severe numerical error will occur if the antenna was mounted on complex platforms.

Although the number of unknowns in the two antenna simulations are relatively small, the computation time will be quite long when the two antennas are numerically analyzed over a wide frequency band. Therefore, the MLFMA is employed in this paper for the analysis of planar monopole antennas mounted on electrically large ground plane [27, 28]. The popular curvilinear Rao-Wilton-Glisson (CRWG) basis function [29] is applied to expand the surface current on the monopole and ground plane. Free-space dyadic Green's function is utilized, which accounts for all the contributions from the surface current on the antenna and large ground plane. Additionally, a novel feed model is presented to precisely model the feed structure. In the new feed model, four basis functions spanning from the monopole segments to the ground plane segments are defined and applied with delta-function generators. Other parameters such as input impedance and VSWR are readily obtained once the current distribution on the feed line is computed. Both of the impedance bandwidth and radiation patterns are numerically and experimentally investigated to demonstrate good performance of the two planar monopoles.

2. ANTENNA DESIGN

In this section, the planar monopole covering the AMPS, GSM900, and DCS band (VSWR < 2) is first described. Then, a new planar monopole antenna with a lower height covering the same frequency band is presented. For the sake of convenience, the two planar monopoles are mentioned as Antenna I and Antenna II throughout this paper, respectively. In the design process, when the primitive geometry of the two planar monopoles are determined, dimensions of the two antennas, such as α, w, and d in Antenna I, are carefully adjusted through an error and trial method for the optimal input impedance over the required frequency band.

The geometry of Antenna I is shown in Figure 1. The planar

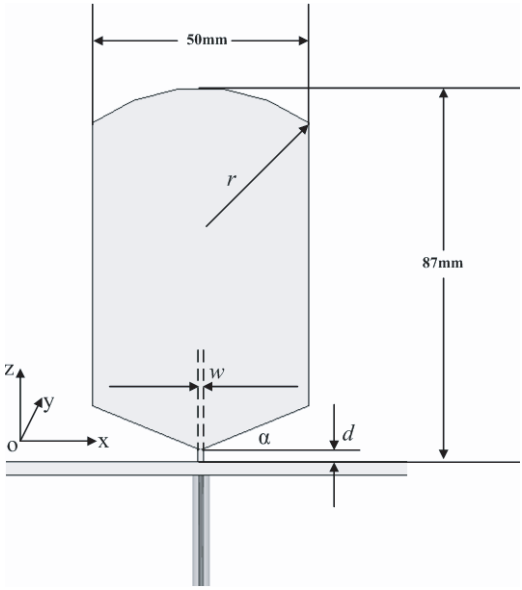

Figure 1. Geometry of Antenna I.

monopole consists of a radiating element and a finite sized ground plane. The radiating element is fabricated from a rectangle copper sheet (transverse size: 50 mm ×87 mm, thickness: 0.5 mm) with bevels cut at its two lower corners, and it is connected to the center conductor of a 50 Ω SMA connector for signal transmission. By adjusting the bevel angle α, feed line width w, and the distance d between the radiating element and the ground plane, good input impedance matching over the frequency band can be achieved. The effect of the bevel angle on the bandwidth has been reported in [30], and the design guidelines are employed in our design. Based on many simulations, the determined optimal dimensions are: $\alpha = 22.3°$, $w = 1.28$ mm, and $d = 3$ mm. Additionally, the top edge of the radiating element is rounded to further improve the impedance matching at higher frequencies, where the current discontinuity at the upper corner is alleviated compared with the monopole presented in [14]. The arc on the top edge is with radius $r = 42$ mm. In this design, the total height of the radiating element mainly controls the lower edge frequency, and the bevels cut in the lower corners would significantly increase the higher edge frequency [31].

The planar monopole antenna with a lower height (Antenna II) is shown in Figure 2; it is also vertically mounted over a finite

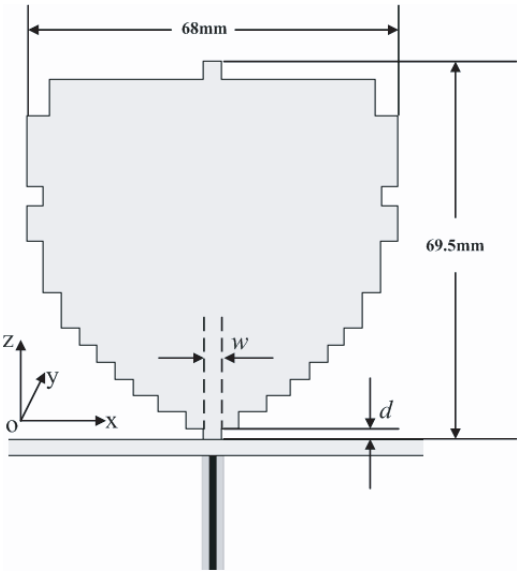

Figure 2. Geometry of Antenna II.

sized ground plane. In both of the planar monopole antennas, an aluminum sheet of 3 mm thickness is used for the finite sized ground plane. With the guidelines and theoretical considerations in [15], one of the optimized monopole antennas (Design 1 in [15]) is taken as the primitive design for our new monopole that covers the AMPS, GSM900, and DCS band. Next, locations and depths for each notch are optimized to achieve a good impedance matching over the frequency band. As stated in [15], the rounded bottom edge in this type of antenna will reduce the severe current discontinuity along the bottom edge, thus the current reflection associated with the discontinuity is suppressed. Furthermore, due to the notches etched along the edges of the monopole, the lateral current components will cancel with each other, which in turn will suppress the cross polarization components. Besides, these notches will also lengthen the current path, thus the physical height of the monopole can be significantly reduced. After an optimization process, the optimal feed line width w and the separation between the bottom of the radiating element and the ground plane d is obtained: $w = 3.2$ mm, $d = 1.8$ mm.

Figure 3 shows the photographs of the two fabricated planar monopole antennas. As illustrated in Figure 3, Antenna I consists of a radiating element and a small finite sized ground plane, while Antenna II is mounted on a large ground plane with dimensions of

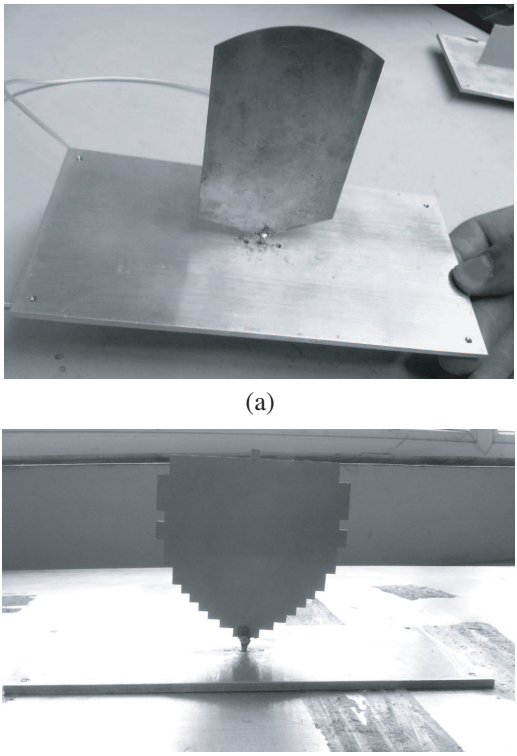

(a)

(b)

Figure 3. Photographs of the two fabricated planar monopole antennas. (a) Antenna I; (b) Antenna II.

500 mm × 500 mm. Since such kinds of planar monopole antennas have great potential use in wireless communication systems with large metal platform, it is necessary to investigate the effect of the large ground plane on the input impedance. In Section 4, the two cases that with and without the large ground plane will be theoretically investigated for the two antennas, and measured results in the large ground plane case will also be presented.

3. THE FEED MODEL

In order to find the true input impedance as would be measured by the network analyzer, a suitable excitation model for producing the impressed field $\vec{E}^{inc}(\vec{r})$ is quite important for MoM analysis of the real

antenna structure. There are at least two issues we should seriously consider in the construction of feed model:

(a) The physical structure near/at the feed point should be modeled exactly in the MoM meshes, since the current distribution at the feed point is significantly influenced by the strong coupling from these structures;

(b) In order to find the true input impedance, the current at the feed point should be depicted precisely, since a tiny error in the current would cause significant errors in the input impedance.

Although there are various wire/surface junction basis functions proposed for the modeling of monopoles mounted on different platforms [32, 33], it is obvious that they have not described the feed structure exactly as what is in practice. Other simplified feed model such as the base-driven model [34, 35], pin-feed model [36], and delta-function generator model [37, 38] are also widely used for the modeling of antenna excitations, but they are so simple that the input impedance would be inaccurate in some cases.

In this paper, a simple yet accurate model is presented to model the feed mechanism of the planar monopoles. Figure 4 illustrates the mesh model of the feed structure, where the surface of the ground plane and feed line is segmented into triangular patches, and there are totally four CRWG elements used to attach the monopole with the ground plane. It is necessary to point out that the 0.5 mm thick antenna is meshed by two sides to caster for the feed model in Figure 4. However, the overall problem is not a closed body; the four sides of the feed line are extended to a large surface, where the large surface is an approximation of the large ground plane. So only EFIE is employed in this paper, and it is not necessary to consider the resonance issue. The model of the delta-function generator is then applied to the four edges that connect the monopole with the ground plane. The contribution of each single edge should be taken into account for the computation of current at the feed point. The formula to calculate the input impedance of the antenna is given by

$$Z_{in} = \frac{V}{\sum_{p=1}^{4} l_p I_p} \tag{1}$$

where V is the feeding voltage on each edge; l_p and I_p represent the edge length and current coefficient of the pth CRWG element. As also depicted in Figure 4, the denominator in (1) accounts for the total current through the feed line of the monopole antenna.

Unlike the base-driven model introduced for the modeling of monopole excitation [32, 34, 35], where a thin strip is used to the thin

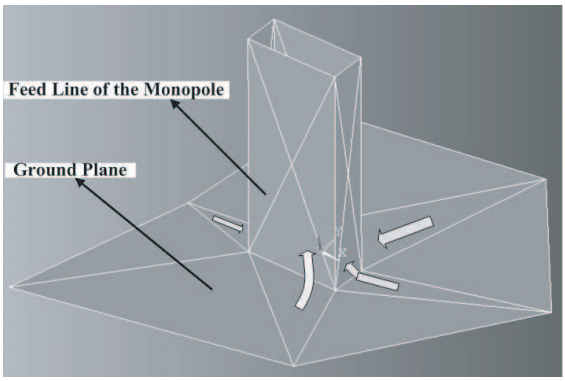

Figure 4. Mesh model of the feed structure.

wire monopole or other kinds of antennas, the feed model in Figure 4 has exactly described the feed structure in real world, and the current flowing from the feed line to the radiation part of the monopole is contributed from all the surface current on the feed line. As compared with the base-driven model in [32, 34, 35], accuracy of the current computed at the feed point is greatly improved, because there is no approximation introduced for the feed structure in this new feed model. Besides, in order to get the true input impedance for more complicated feed structures, the meshes on the junction part is possible to be refined and more CRWG elements can be introduced at the junction interface to compute the current at the feed point accurately. On the other hand, as the mesh density is further enhanced at the feed structure, it is worthwhile to consider the low frequency breakdown problem, since MLFMA will suffer from numerical instability, which is due to the inability of MLFMA in the handling of low frequency interaction. Recently, efficient techniques such as the nondirective stable plane wave MLFMA [39] have been proposed to evaluate the low frequency interactions in structures containing subwavelength geometrical detail. Thus, if the grids on the feed structure are further refined, these kinds of techniques can be employed to avoid the mentioned problems.

4. NUMERICAL AND EXPERIMENTAL RESULTS

To demonstrate the performance of the two planar monopoles, the two monopoles are analyzed by the MLFMA; measured results including VSWR and radiation characteristics are also presented to validate the effectiveness of the feed model in MLFMA. Effect of the large ground plane (500 mm $\times$ 500 mm) on the impedance bandwidth is also

investigated.

In the MLFMA model of Antenna I, mesh density for the radiating element and large ground plane are $\lambda_H/7.5$ and $\lambda_H/12$, respectively, where λ_H is the wavelength at the highest frequency of $f_H = 2\,\text{GHz}$. The mesh refinement on the radiating element is quite useful, since it provides an adequately precise model for the faster current variation appearing in the feed structure and vertexes. In this model, there are totally 3520 basis functions defined on the radiating element and large ground plane, from which there are 2062 basis functions defined to expand the surface current on the large ground plane. Delta-function generators are applied across the common edges in the attachment between the feed line and the finite sized ground plane. The error bound of 0.01 is used for the GMRES iterative method, which is sufficient for the radiation problems discussed here. The electric size of the finest cube is set to be 0.3λ, and the mode number L is calculated through the semi-empirical formula

$$L \approx kd + 2\ln(\pi + kd) \tag{2}$$

where the factor in front of the $\ln(\cdot)$ term is dependent on the accuracy, and d is the summation of two local vectors in the MLFMA formulations.

The simulated VSWR over the frequency band for Antenna I with and without large ground plane is shown in Figure 5(a). From the results, it is clearly seen that the large ground plane has lowered the VSWR significantly at lower frequencies. Wide impedance bandwidth (VSWR < 2) is observed over the AMPS, GSM900, and DCS band.

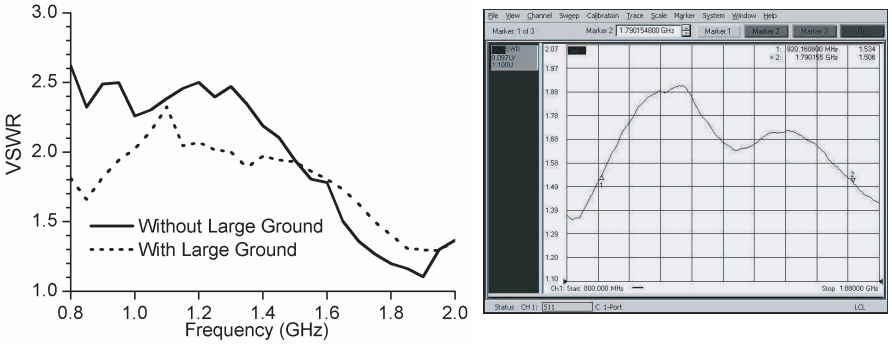

Figure 5. Simulated and measured VSWR of Antenna I. (a) Simulated VSWR for antenna with and without large ground plane; (b) Measured VSWR for Antenna I mounted on a large ground plane.

Figure 5(b) displays the measured VSWR for Antenna I with large ground plane. It can be observed that there is some slight discrepancy between the numerical simulated and measured VSWR. However, both of the numerical and experimental results demonstrate that the planar monopole with a large ground plane has a wide impedance bandwidth over (VSWR < 2) the AMPS, GSM900, and DCS. The main factor behind the discrepancy is the difference between the simulation model and the model in real world. Specifically, the feed model introduced in this paper is an approximate model of the feed structure in practice, although it is more precise than those in the listed references and can provide a performance prediction for the planar monopole with sufficient accuracy. Secondly, the ground plane with a thickness of 3 mm is replaced by a surface of infinitesimal thickness. The equipment error will also contribute to such differences.

The radiation characteristics of Antenna I with a large ground plane are also studied. For the sake of brevity, only radiation patterns at 900 MHz and 1800 MHz are presented. For other frequencies, radiation patterns are about the same as those at 900 MHz and 1800 MHz. Figures 6(a) and (b) show the measured E-plane radiation patterns in the xoz and yoz planes, and Figure 6(c) plots the measured radiation patterns in the H-plane (xoy plane). Numerically calculated radiation patterns from MLFMA are presented for comparison. It is firstly seen that there are typical monopole patterns in the two E-planes. Besides, good omnidirectional radiation characteristics (defined here for maximum gain variation less than 3 dB) in the H-plane has also been achieved for Antenna I. Apart from the difference between the simulation model and model in practice, the slight discrepancy between the simulated and measured radiation patterns also results from the alignment errors during the measurement process. For frequencies ranging from 800 MHz to 1880 MHz, antenna gain is increased monotonically from about 4.0 to 7.0 dBi, which has not been shown in Figure 6 for comparison of the numerical and experimental results.

Similarly, performance of Antenna II is also investigated numerically and experimentally. In the MLFMA model, the same mesh density as in Antenna I is applied to the radiating element and large ground plane of Antenna II. The number of basis functions defined on the radiating element and large ground are 1851 and 2062, respectively. The same error bound in the GMRES iterative method is set to ensure the accuracy of the solved current coefficient. Detailed information of the MLFMA is kept the same as in the first antenna's analysis. Effect of the large ground plane on the input impedance bandwidth is then investigated using the MLFMA. The simulated VSWRs in

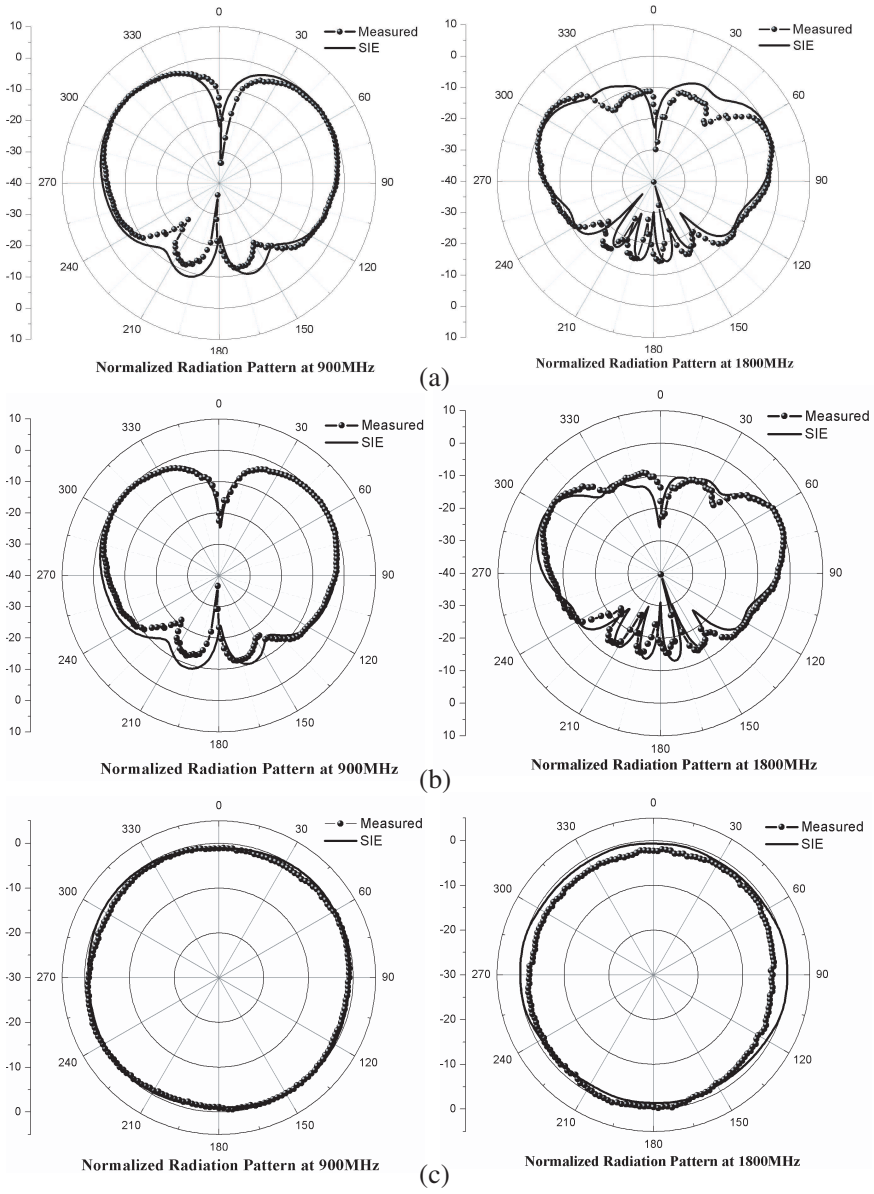

Figure 6. Simulated and measured radiation patterns for Antenna I mounted on a large ground plane. (a) E_θ in the xoz plane; (b) E_θ in the yoz plane; (c) E_θ in the xoy plane.

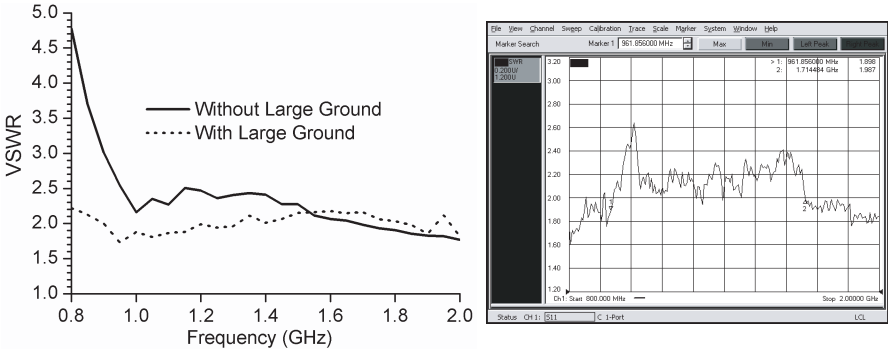

Figure 7. Simulated and measured VSWR of Antenna II. (a) Simulated VSWR for antenna with and without large ground plane; (b) Measured VSWR for Antenna II mounted on a large ground plane.

Figure 7(a) again demonstrate that the large ground plane will improve the impedance matching at lower frequencies. Measured VSWR for Antenna II with a large ground plane is presented in Figure 7(b). Both of the simulated and measured results show that the VSWR remains below 2 : 1 for the AMPS, GSM900, and DCS band.

Figure 8 presents the measured radiation patterns of Antenna II, where the effect of the large ground plane is also included. Simulated radiation patterns are shown for comparison. Again, typical monopole patterns are observed in the E-planes for frequencies of 900 MHz and 1800 MHz (see Figures 8(a) and (b)), and omnidirectional radiation patterns are observed in the H-plane. We can also observe that there is also some discrepancy between the MLFMA simulated and experimentally measured results. It is feasible to say that this discrepancy also results from the errors introduced in the measurement process and the approximate model in the MLFMA simulation. Note that the total height of Antenna II is only $0.19\lambda_L$, which is much lower than the height of Antenna I $0.24\lambda_L$ (λ_L is the wavelength at lower edge of the AMPS band). As expected from the relatively compact size of Antenna II, gain of Antenna II would be lower than Antenna I. Numerical and experimental results demonstrate that the gain of Antenna II increases monotonically from about 2.5 to 6.3 dBi in the frequency range of 800–1880 MHz, which is slightly lower than that of Antenna I.

Finally, time and memory requirements of the MLFMA are compared with those in MoM. Table 1 summarizes the computational time and memory requirements for the two antenna simulations when

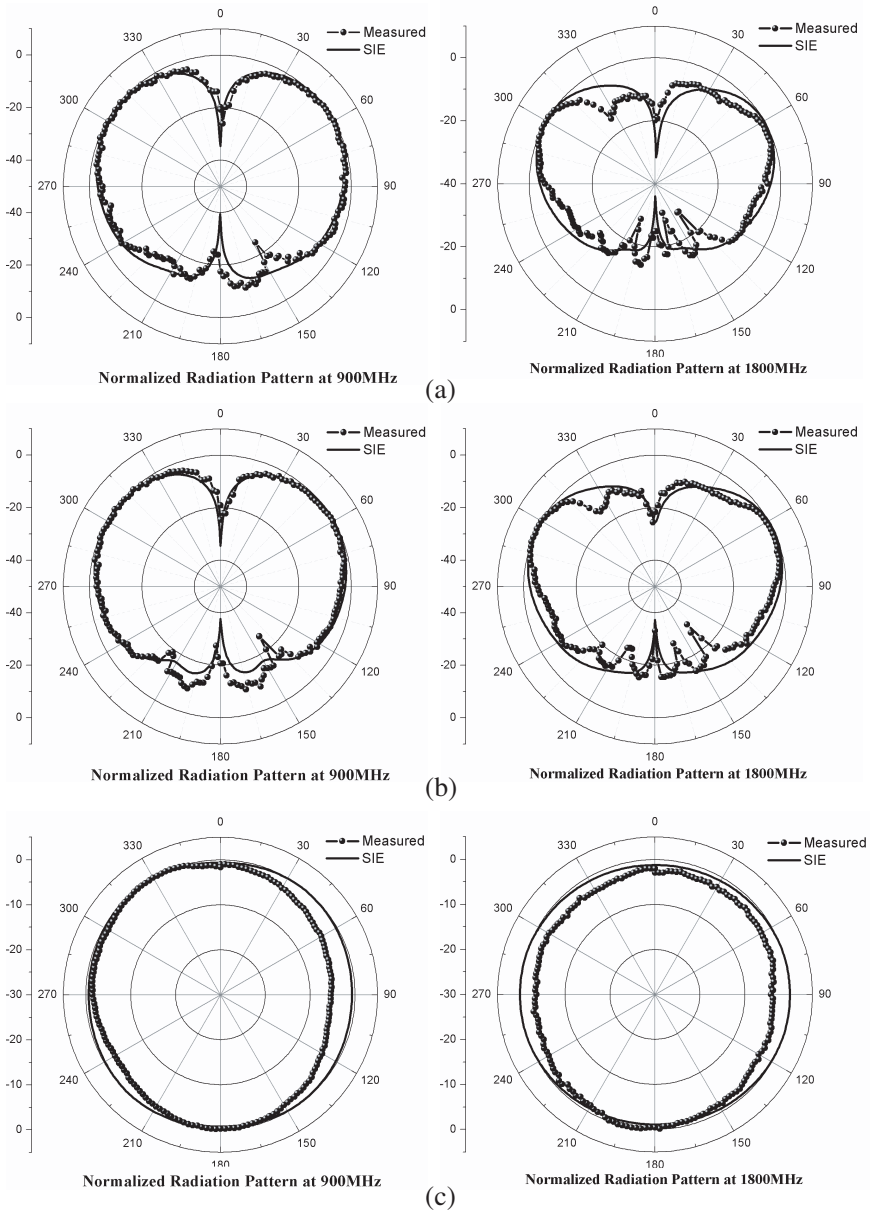

Figure 8. Simulated and measured radiation patterns for Antenna II mounted on a large ground plane. (a) E_θ in the xoz plane; (b) E_θ in the yoz plane; (c) E_θ in the xoy plane.

MoM and MLFMA are applied, respectively. The terms listed in Table 1 correspond to the simulations at $f = 1800$ MHz. As can be seen, the memory requirement of MLFMA is significantly reduced, and the time consumption is reduced to only about 60% of that in MOM. Therefore, the total time consumed could also be reduced significantly if the simulations are carried out in wideband problems. In this paper, frequency points are sampled over a wide frequency band of 800–2000 MHz with a step of 50 MHz. This is also the motivation we employed the MLFMA for the electrically small problems discussed herein.

Table 1. Comparison of the computational resource consumption in MoM and MLFMA.

	Antenna I		Antenna II	
	MoM	MLFMA	MoM	MLFMA
Computational time	1161 s	785 s	1174 s	723 s
Memory requirement	101.296 MB	31.838 MB	127.43 MB	45.892 MB

5. CONCLUSION

Two wideband planar monopoles attached to finite sized ground planes are designed, analyzed, and fabricated. Both of the simulated and measured results showe that the two monopoles are capable to cover the AMPS, GSM900, and DCS band. In the whole operating frequency, both of the monopoles can provide a nearly omnidirectional radiation pattern in the azimuth plane. With relatively low profile, the two compact planar monopoles have great potential use in multi-band wireless communication systems such as receivers on vehicles. Besides, a new feed model has been introduced in MLFMA for the analysis of 3D radiation problems. The MLFMA simulated results agree well with those experimentally measured ones, thus the effectiveness of the MLFMA code as well as the new feed model is demonstrated. Even though the formulations stated are only applicable to perfect electric conducting objects, they could be easily extended to other radiation problems involving dielectric bodies, such as microstrip antennas and dielectric resonator antennas.

ACKNOWLEDGMENT

This work was supported in part by the New Century Excellent Talent Program in China (Grant No. NCET-06-0809), and in part by the 111 project of China (Grant No. B07046).

REFERENCES

1. Row, J. and S. Chen, "Wideband monopolar square-ring patch antenna," *IEEE Trans. Antennas Propagat.*, Vol. 54, No. 4, 1335–1339, Apr. 2006.
2. Guo, Y., M. Chia, Z. Chen, and K. Luk, "Wide-band L-probe fed circular patch antenna for conical-pattern radiation," *IEEE Trans. Antennas Propagat.*, Vol. 52, No. 4, 1115–1116, Apr. 2004.
3. Ravipati, C., "Compact circular microstrip antenna for conical patterns," *Proc. IEEE Int. Symp. Antennas and Propagation*, Vol. 4, 3820–3823, Monterey, CA, June 2004.
4. Al-Zoubi, A., F. Yang, and A. Kishk, "A low-profile dual-band surface wave antenna with a monopole-like pattern," *IEEE Trans. Antennas Propagat.*, Vol. 55, No. 12, 3404–3412, Dec. 2007.
5. Yang, F., Y. Rahmat-Samii, and A. Kishk, "Low-profile patch-fed surface wave antenna with a monopole-like radiation pattern," *IET Microw. Antennas Propagat.*, Vol. 1, No. 1, 261–266, Feb. 2007.
6. Dubost, G., and S. Zisler, *Antennas a Large Band*, 128–129, Masson, New York, 1976.
7. Hammoud, M., P. Poey, and F. Colombel, "Matching the input impedance of a broadband disc monopole," *Electron. Lett.*, Vol. 29, No. 4, 406–407, Feb. 1993.
8. Wu, Q., R. Jin, J. Geng, and M. Ding, "Pulse preserving capabilities of printed circular disk monopole antennas with different grounds for the specified input signal forms," *IEEE Trans. Antennas Propagat.*, Vol. 55, No. 10, 2866–2872, Oct. 2007.
9. Liang, J., L. Guo, C. C. Chiau, X. Chen, and C. G. Parini, "Study of CPW-fed circular disc monopole antenna for ultra wideband applications," *IEE Proc. Microw. Antennas Propagat.*, Vol. 152, No. 6, 520–526, Dec. 2005.
10. Ammann, M. and Z. Chen, "A wide-band shorted planar monopole with bevel," *IEEE Trans. Antennas Propagat.*, Vol. 51, No. 4, 901–903, Apr. 2003.
11. Cerretelli, M., V. Tesi, and G. Gentili, "Design of a shape-constrained dual-band polygonal monopole for car roof

mounting," *IEEE Trans. Vehicular Technol.*, Vol. 57, No. 3, 1398–1403, May 2008.

12. Lin, S., "A low-profile folded planar monopole antenna for wireless communication," *Microw. Opt. Technol. Lett.*, Vol. 36, No. 1, 46–48, Jan. 2003.
13. Su, S., K. Wong, and C. Tang, "Band-notched ultra-wideband planar-monopole antenna," *Microw. Opt. Technol. Lett.*, Vol. 44, No. 3, 217–219, Feb. 2005.
14. Qiu, J., Z. Du, J. Lu, and K. Gong, "A case study to improve the impedance bandwidth of a planar monopole," *Microw. Opt. Technol. Lett.*, Vol. 45, No. 2, 124–126, Apr. 2005.
15. Kerkhoff, A., R. Rogers, and H. Ling, "Design and analysis of planar monopole antennas using a genetic algorithm approach," *IEEE Trans. Antennas Propagat.*, Vol. 52, No. 10, 2709–2718, Oct. 2004.
16. Zhou, H., Q. Liu, Y. Yin, and W. Wei, "Study of the band-notch function for swallow-tailed planar monopole antennas," *Progress In Electromagnetics Research*, PIER 77, 55–65, 2007.
17. Antonino-Daviu, E., M. Cabedo-Fabres, M. Ferrando-Bataller, and A. Valero-Nogueira, "Wideband double-fed planar monopole antennas," *Electron. Lett.*, Vol. 39, No. 23, 1635–1636, Nov. 2003.
18. Wong, K., C. Wu, and S. Su, "Ultrawide-band square planar metal-plate monopole antenna with a trident-shaped feeding strip," *IEEE Trans. Antennas Propagat.*, Vol. 53, No. 4, 1262–1269, Apr. 2005.
19. Anob, P. V., K. P. Ray, and G. Kumar, "Wideband orthogonal square monopole antennas with semi-circular base," *Proc. IEEE Int. Symp. Antennas and Propagation*, Vol. 3, 294–297, Boston, MA, July 2001.
20. Chen, Z., "Broadband roll monopole," *IEEE Trans. Antennas Propagat.*, Vol. 51, No. 11, 3175–3177, Nov. 2003.
21. Su, S. and K. Wong, "Broadband omnidirectional U-shaped metal-plate monopole antenna," *Microw. Opt. Technol. Lett.*, Vol. 44, No. 4, 365–369, Feb. 2005.
22. Thiele, G. and T. Newhouse, "A hybrid technique for combining moment methods with the geometrical theory of diffraction," *IEEE Trans. Antennas Propagat.*, Vol. 23, No. 1, 62–69, Jan. 1975.
23. Awadalla, K. and T. Maclean, "Input impedance of a monopole antenna at the center of a finite ground plane," *IEEE Trans. Antennas Propagat.*, Vol. 26, No. 2, 244–248, Mar. 1978.
24. Richmond, J., "Monopole antenna on circular disk over flat

earth," *IEEE Trans. Antennas Propagat.*, Vol. 33, No. 6, 633–637, June 1985.

25. Richmond, J., "Monopole antenna on circular disk," *IEEE Trans. Antennas Propagat.*, Vol. 32, No. 12, 1282–1287, Dec. 1984.
26. Cook, G. and S. Khamas, "Fast approximate moment method model for monopole arbitrarily positioned on circular ground plane," *Electron. Lett.*, Vol. 29, No. 2, 223–224, Jan. 1993.
27. Song, J., C. Lu, and W. Chew, "Multilevel fast multipole algorithm for electromagnetic scattering by large complex objects," *IEEE Trans. Antennas Propagat.*, Vol. 45, No. 10, 1488–1493, Oct. 1997.
28. Ergül and L. Gürel, "Modelling and synthesis of circular-sectoral arrays of log-periodic antennas using multilevel fast multipole algorithm and genetic algorithms," *Radio Science*, 42, RS3018, June 2007.
29. Brown, W. and D. Wilton, "Singular basis functions and curvilinear triangles in the solution of the electric field integral equation," *IEEE Trans. Antennas Propagat.*, Vol. 47, No. 2, 347–353, Feb. 1999.
30. Ammann, M. and Z. Chen, "Wideband monopole antennas for multi-band wireless systems," *IEEE Antennas Propagat. Mag.*, Vol. 45, No. 2, 146–150, Apr. 2003.
31. Evans, J. and M. Amunann, "Planar trapezoidal and pentagonal monopoles with impedance bandwidths in excess of 10 : 1," *Proc. IEEE Int. Symp. Antennas and Propagation*, Vol. 3, 1558–1561, Orlando, FL, July 1999.
32. Matthews, J. and G. Cook, "An efficient method for attaching thin wire monopoles to surfaces modeled using triangular patch segmentation," *IEEE Trans. Antennas Propagat.*, Vol. 51, No. 7, 1623–1629, July 2003.
33. Yuan, N., T. Yeo, X. Nie, Y. Gan, and L. Li, "Analysis of probe-fed conformal microstrip antennas on finite grounded substrate," *IEEE Trans. Antennas Propagat.*, Vol. 54, No. 2, 554–563, Feb. 2006.
34. Makarov, S., "MoM antenna simulations with Matlab: RWG basis functions," *IEEE Antennas Propagat. Mag.*, Vol. 43, No. 5, 100–107, Oct. 2001.
35. Makarov, S., *Antenna and EM Modeling with MATLAB*, Wiley, Hoboken, NJ, 2002.
36. Liu, X., C. Liang, and X. Zhao, "Analysis of waveguide slot antennas using MLFMA," *Microw. Opt. Technol. Lett.*, Vol. 50,

No. 1, 65–68, Jan. 2008.

37. Namkung, J., E. Hines, R. Green, and M. Leeson, "Probe-fed microstrip antenna feed point optimization using a genetic algorithm and the method of moments," *Microw. Opt. Technol. Lett.*, Vol. 49, No. 2, 325–329, Feb. 2007.
38. Lim, C., L. Li, and M. Leong, "Method of moments analysis of electrically large thin hexagonal loop transceiver antennas: Near- and far-zone fields," *Progress In Electromagnetics Research*, PIER 30, 251–271, 2001.
39. Bogaert, I., J. Peeters, and F. Olyslager, "A nondirective plane wave MLFMA stable at low frequencies," *IEEE Trans. Antennas Propagat.*, Vol. 56, No. 12, 3752–3767, Dec. 2008.